ELSEVIER

Journal of Alloys and Compounds 293–295 (1999) 608–612

Journal of ALLOYS AND COMPOUNDS

Effects of cooling rate during casting on performance of metal hydride electrodes and nickel–metal hydride batteries

L.Y. Zhang[a,*], Michael Klein[a], Bob Czajkowski[a], Lee Huston[a], Rolf Pechloff[b], Demin Chen[c], Ke Yang[c]

[a]*Energizer Power Systems, P.O. Box 147114, Gainesville, FL 32614-7114, USA*
[b]*GfE Metalle und Materialien Gmbh, Hofener Strasse 45, D-90431 Nuremberg, Germany*
[c]*Institute of Metal Research, Academia Sinica, 72 Wenhua Road, Shenyang 110015, PR China*

Abstract

In this work, three $Mm(Ni–Co–Mn–Al)_5$ alloys with the same formula were produced by vacuum induction melting and casted at different cooling rates: normal cooling, fast cooling, rapid quenching. In addition, a portion of the rapidly quenched alloy was annealed. The crystallographic and structural properties and the electrochemical performance of these materials were characterized. For all the as-cast alloys, cooling rate did not significantly affect their activation process and cycle life. In contrast, the alloy, which was rapidly quenched and then annealed, displayed a longer cycle life. However, it required a long activation process to achieve its maximum capacity. The effects of metallurgical processes on the sealed cell performance such as cycle life, internal gaseous pressure after charging, and storage behavior after formation were also examined.

Keywords: Hydrogen storage alloy; MH electrode; Nickel–metal hydride batteries

1. Introduction

The multicomponent AB_5 type hydrogen storage alloy is considered the most suitable material for the metal hydride (MH) electrode. It was reported [1–3] that for an AB_5 type alloy, its microstructure plays a key role in the alloy's performance. The microstructure involves phase distribution, grain size, element segregation, chemistry and structure of grain boundaries, etc. These features are controlled by metallurgical conditions of alloy preparation. In this work, electrochemical performance of $Mm(NiCoMnAl)_5$ type alloys with different rate of solidification available in industrial equipment was investigated from the viewpoint of battery applications. The influence of metallurgical processes on the alloy's properties and the performance of both MH electrodes and sealed nickel–metal hydride cells (Ni–MH) is presented.

2. Experimental

Three alloy samples used in this study were produced by melting of elemental raw materials of commercial purity (99+%) using 1500 kg vacuum induction furnace at Gesellschaft fuer Elektrometallurgie (GfE) in Germany. All the alloys had the same nominal composition $MmNi_{3.6}Co_{0.7}Mn_{0.3}Al_{0.4}$, where Mm is a La-rich mischmetal with approximately 50% La. The melted alloys were solidified at three cooling rate: normal cooling (NC), fast cooling (FC), and rapid quenching (RQ), which were controlled by the geometry and thickness of the ingots. A part of RQ alloy was annealed (RQ/HT) at 950°C for 12 h (Table 1). Pressure–composition isotherms (*PCT*s) on hydrogen desorption were procured at 45°C using Sievert-s'-type apparatus. Lattice constants of both host alloys and their hydrides (1 atm) were determined using standard powder diffraction techniques in the Institute of Metal Research (IMR), Chinese Academy of Sciences in China.

The alloy ingots were mechanically pulverized to <75 μm powder. MH electrodes for the activation process test were made by mixing 250 mg of MH powder with 250 mg of INCO nickel powder (type 287), then cold pressed to form a pellet with a diameter of 8 mm and a thickness of about 1.5 mm. Pasted MH electrodes of thin nickel-plated perforated steel substrate were fabricated for cycle life test. A half-cell was constructed using MH as working electrode, a sintered $Ni(OH)_2/NiOOH$ as counter electrode

*Corresponding author.

0925-8388/99/$ – see front matter
PII: S0925-8388(99)00352-7

Table 1
Metallurgical processes of the AB_5 alloys

Alloy		Thickness (mm)	Cooling rate (in order; °C/S)	Remarks
NC	Normal cooling	30	10^1	As-cast
FC	Fast cooling	10	10^2	As-cast
RQ	Rapid quench	1	10^3	As-cast
RQ/H/T	RQ and annealed	1	10^3	Annealed

and a Hg/HgO reference electrode in 30 wt.% KOH electrolyte solution.

AA NiMH cells were assembled by winding thin planar $Ni(OH)_2$ sinter-type electrodes and the pasted MH electrodes between a layer of battery-grade separator. The cell capacity was set by the positive electrode at approximately 1100 mAh. During cycling test, the cells were 1 C rate (1100 mA) charge to a negative change in voltage ($-\Delta V$) or 38°C was reached (whichever comes first), followed by a C/10 charge rate (approximately 2 h) to fill a 3-h test time window. Cells were rested for 2 min after charge and then discharged at 1 C to 0.9 V followed by a 1-h rest. The cells' internal pressure during charge and discharge were monitored in situ. The gas chemistry for cells charged at 1 C rate for 70 min were also analyzed.

For cell storage evaluation, 3.0 AH 4/3 A NiMH cells were assembled in a similar way as that for the AA cells, but the positive electrodes were Ni-foam pasted $Ni(OH)_2$.

3. Results and discussion

3.1. Alloy characterization

The crystal structure and homogeneity of the prepared compounds were examined by powder X-ray diffraction with CuKα radiation. Both host alloys and their hydrides were indexed with $CaCu_5$ type hexagonal structure. The lattice constants, a/c ratio and percent change in unit cell volume upon hydrogenation are listed in Table 2. The lattice parameters and unit volume of the as-cast alloys are nearly equal independent of the quench rate. All the hydrides exhibited about ~18% lattice expansion, while the RQ/HT alloy expanded by 19%, which may indicate either a change in mechanical strength or hydrogen solubility in the hydride phase. The a/c values of the hydrides are larger than their parent alloys indicating strong anisotropic behavior.

It was revealed from SEM analysis and X-ray mapping images (Fig. 1) that the normal cooling displays clear network Mn segregation as compared with the FC and RQ alloys. Fig. 2 displays isotherms of gas-phase desorption at 45°C. All as-cast alloys exhibit similar behavior, while the RQ/HT alloy displays a flatter plateau. The upward slope of the isotherms for the as-cast alloys may be attributed to the chemical inhomogeneity and lattice strain.

3.2. Activation and corrosion resistance

Activation processes were evaluated using pellet half cells. The cells were charged at 100 mA/g for 4 h, and discharged at the same rate to 0.7 V (vs. Hg/HgO). As shown in Fig. 3, in order to achieve their maximum capacity, all as-cast electrodes need three cycles, however the RQ/HT electrode needs six cycles.

The cyclic life for the pasted electrodes ($T=21$°C) is displayed in Fig. 4. All the as-cast electrodes exhibit similar capacity trend, while the RQ/HT electrode shows a slower degradation rate. Using regression statistics, the degradation rate was calculated and illustrated in Table 3. All the as-cast alloys have degradation rates of $\sim 2\times10^{-2}$ mAh/g per cycle, while the RQ/HT exhibits the best corrosion resistance with the rate of $\sim 1\times10^{-2}$ mAh/g per cycle.

3.3. Sealed cell performance

3.3.1. Cycle life

Mid-point voltage (MPV) vs. Cycle number of cycle life tests on AA cells are illustrated in Fig. 5, which displays the same trend as the cell capacities. The RQ/HT alloy exhibits superior cycle life to all the as-cast alloys, which is in agreement with the half cell test (see Fig. 4). It is an

Table 2
Crystal structure parameters of the host alloys and their hydrides

Alloy	a_o (nm)	c_o (nm)	a_o/c_o	Hydride	a_h (nm)	c_h (nm)	a_h/c_h	$\Delta V/V$ (%)
NC	0.500	0.406	1.23	NC–H	0.533	0.422	1.26	18.0
FC	0.500	0.405	1.23	FC–H	0.533	0.420	1.27	17.9
RQ	0.501	0.406	1.24	RQ–H	0.533	0.423	1.26	17.8
RQ/HT	0.501	0.405	1.24	RQ/HT–H	0.534	0.425	1.26	18.9

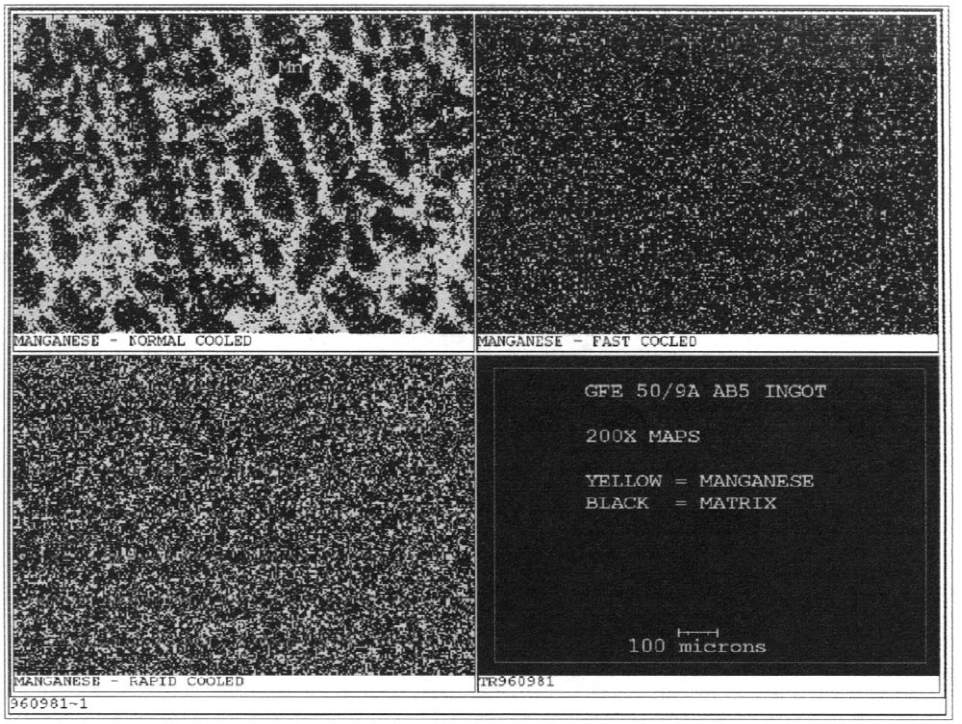

Fig. 1. SEM images of NC, FC and RQ alloys. The network type structure in the NC alloy shows clearly Mn segregation as compared with FC and RQ alloys.

indication that the MH electrode corrosion resistance, and in turn to the cell cycle life could be improved with the alloy heat treatment.

3.3.2. Internal pressure

The internal pressures of gases evolved from charging of the AA cells were measured. Fig. 6 shows the in situ monitoring of the internal pressure as well as the cell voltage during the charge, rest and discharge process on the 30th cycle for cells of NC and RQ/HT. The cell voltages exhibit very similar behavior, while the RQ/HT cell displays lower pressure than the NC cell. Fig. 7 shows the partial gas pressure after the cells were charged at 1 C rate for 70 min.

3.3.3. Storage

3.0 AH 4/3A cells were given five charge and discharge cycles, and then stored at 45°C for 90 days, in either the charged and discharged state. The cell voltage was monitored during the shelf time, and then the cells were cycled to evaluate their capacity and capacity recovery. All the charged cells show the same trends in both cell voltage and capacity recovery. However, for the discharged cells as shown in Figs. 8 and 9, the alloys of NC and RQ/HT

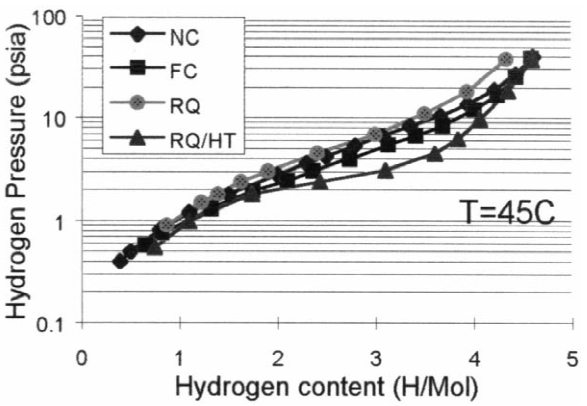

Fig. 2. Gas phase desorption isotherms of theAB_5 alloys at 45°C with different metallurgical processing.

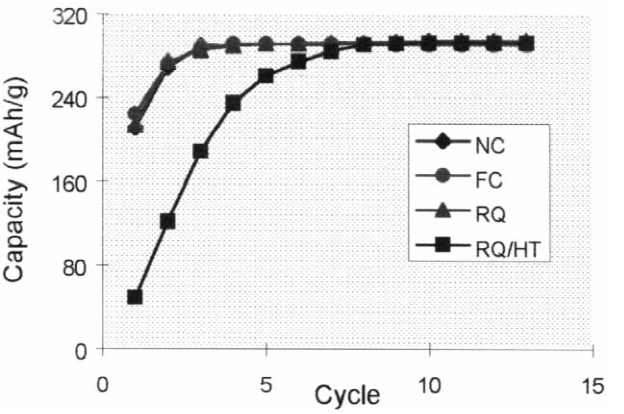

Fig. 3. Activation processes of pellet MH electrodes.The cells were charged and discharged at a rate of 100 mA/g.

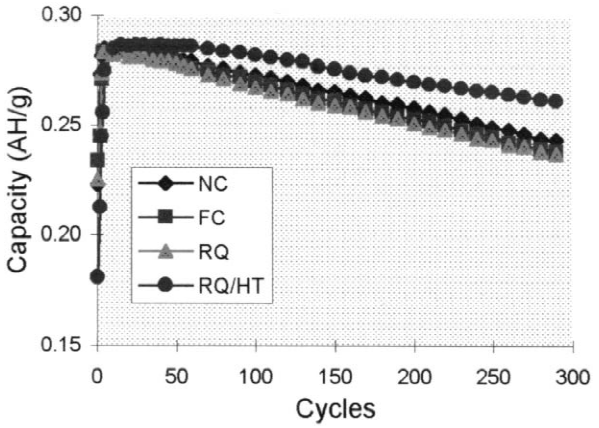

Fig. 4. Cyclic life for pasted MH electrodes. The pasted electrodes were charged for 2.5 h and discharged to 0.7 V (Hg/HgO) at a rate of 150 mA/g.

Table 3
Degradation rates of the MH electrodes

Alloy	NC	FC	RQ	RQ/HT
Degradation rate (mAh/g·cycle)	1.8×10^{-2}	1.9×10^{-2}	2.1×10^{-2}	9.7×10^{-3}

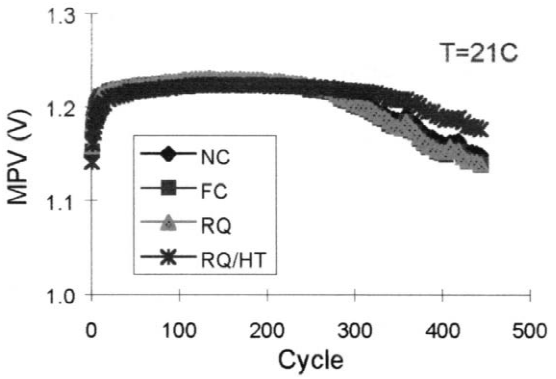

Fig. 5. Cycling life for AA cells containing AB_5 alloys with different metallurgical treatments.

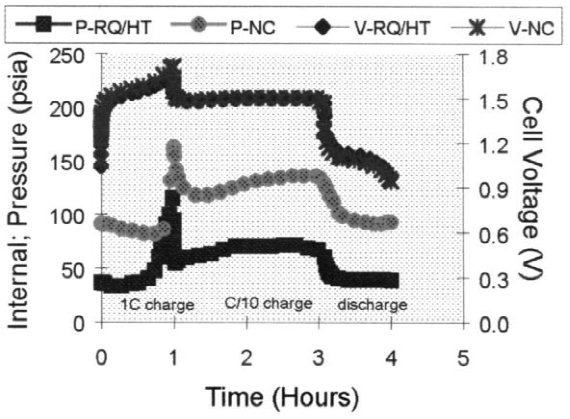

Fig. 6. In situ monitoring of AA cell voltage and pressure during the 30th cycle for cells of NC and RQ/HT alloys.

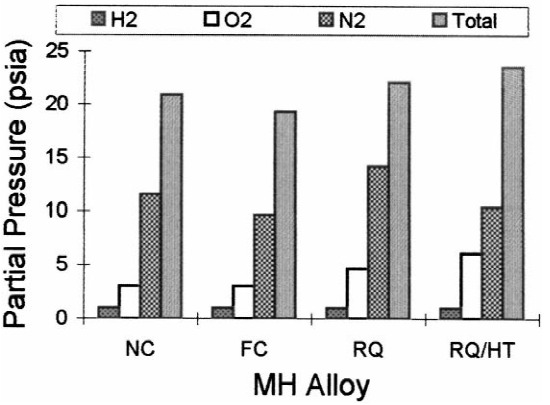

Fig. 7. Internal pressure of gases measured after the AA cells were charged for 70 min at 1 C rate and removed from charge immediately.

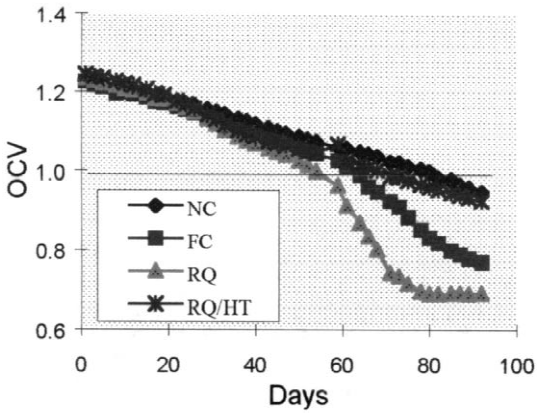

Fig. 8. Voltage of discharged Ni-foam 4/3A cells vs. time during storage at 45°C.

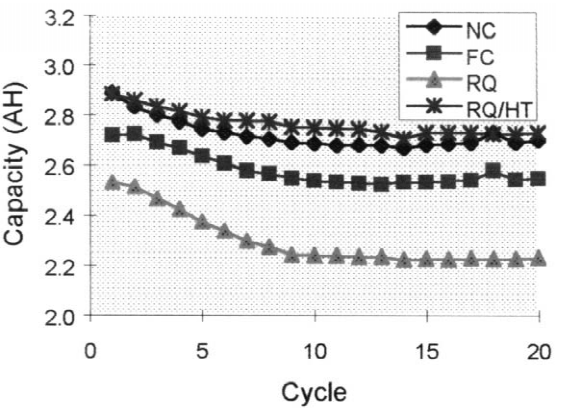

Fig. 9. Capacity recovery for the discharged 4/3A cells after 90 days storage at 45°C.

exhibit similar behavior, while the FC and RQ display early voltage drop and much lower capacity recovery. The mechanism of the storage behavior is not clear yet. It may be related to the migration of metallic ions from the MH electrode to the Ni-electrode [4].

4. Conclusions

Our studies have found that for the as-cast $Mm(NiCoMnAl)_5$ alloys, the cooling rate during cast in order of 10 to 1000°C/S does not show significant influence in activation processes, alloy corrosion resistance, and cycle life. However, the heat treatment may improve the alloy corrosion resistance, reduces internal gas pressure and extends cell cyclic life. Effects of metallurgical conditions on sealed cell storage can not be explained with standard analytical techniques (XRD, microstructure, SEM, etc.).

References

[1] T. Sakai, H. Yoshinaga, H. Miyamura, N. Kuriyama, H. Ishikawa, J. Alloys Compd. 180 (1992) 37–54.
[2] T. Sakai, H. Miyamura, N. Kuriyama, Z. Phys. Chem. NF 183 (1994) 333–346.
[3] L.Y. Zhang, T. O'Hara, G. Michal, in: P.D. Bannet, T. Sakai (Eds.), Proc. Symp. On Hydrogen and Metal Hydride Batteries, 1994, pp. 45–56.
[4] D. Singh, T. Wu, M. Wendling, P. Bendale, J. Ware, L.Y. Zhang, Mat. Res. Soc. Symp. Proc. 496 (1998) 25–36.